



PERGAMON

Journal of Geodynamics 32 (2001) 467–486

---

---

JOURNAL OF  
**GEODYNAMICS**

---

---

www.elsevier.com/locate/jgeodyn

# Thermal state of the Campi Flegrei caldera inferred from seismic attenuation tomography

Salvatore de Lorenzo<sup>a,\*</sup>, Paolo Gasparini<sup>b</sup>, Francesco Mongelli<sup>a</sup>, Aldo Zollo<sup>b</sup>

<sup>a</sup>*Dipartimento di Geologia e Geofisica, Università di Bari, Via Orabona 4, 70125 Bari, Italy*

<sup>b</sup>*Dipartimento di Scienze Fisiche, Università di Napoli "Federico II", Italy*

Received 11 April 2000; received in revised form 15 December 2000; accepted 5 February 2001

---

## Abstract

A three-dimensional  $Q_p$  image of the Campi Flegrei caldera between 0 and 3 km of depth has been inferred by the inversion of P rise time and pulse width data of 87 local earthquakes recorded during the last bradiseismic crisis by a local array deployed in the area by the University of Wisconsin. The availability of both thermal measurements in 5 deep boreholes and of a heat flow surface map of the area allowed us to calibrate the local temperature  $F$  vs.  $Q_p$  relationship. The comparison of  $Q_p$ ,  $V_p$  and  $V_p/V_s$  images, combined with hydrogeological and geochemical data from deep boreholes, allowed us to distinguish some low- $Q_p$  anomalies related to the presence of fluids in the rocks from a deep low- $Q_p$  anomaly related to the conductive cooling of a magma reservoir. The deep anomaly is located in the same zone where several authors believe that the volcanic and magmatic activity migrated after the Neapolitan Yellow Tuff eruption. Moreover this anomaly includes the area where the existence of a magma chamber at depth between 4 and 5 km was inferred by an active seismic experiment. © 2001 Published by Elsevier Science Ltd. All rights reserved.

---

## 1. Introduction

Campi Flegrei is a resurgent caldera located inside the Campanian Plain, a graben-like structure at the eastern margin of the Tyrrhenian Sea. The caldera formation is believed to be related to two main explosive eruptions. The oldest one occurred 37–39 kyears ago (Civetta et al., 1997; Di Vito et al., 1999) and erupted about 200 km<sup>3</sup> of dense rock equivalent (Wohletz et al., 1999), producing a huge ignimbrite formation (Campanian ignimbrite or Campanian grey tuff). The youngest one is dated at about 12 kyears, and erupted about 40 km<sup>3</sup> of dense rock equivalent producing a thick tuff formation (Neapolitan yellow tuff) (Orsi et al., 1996). The most recent

---

\* Corresponding author. Tel.: +39-805-544-2583; fax: +39-805-544-2625.

E-mail address: delorenzo@geo.uniba.it (S. de Lorenzo).

eruptive activity is mainly phreatomagmatic. It is confined within the most recent caldera and the main eruptive episodes are clustered at 9.5–12, 8–9 and 4–5 kyears ago. The last eruption occurred in 1538 and formed a 150 m-high spatter cone (Mt. Nuovo).

Archeological and historical evidence indicates that the caldera bottom has been slowly sinking in the last 2000 years. The sinking trend was interrupted at least 40 years before the Mt. Nuovo eruption, when historical documents clearly indicate that an inflation was underway. The total uplift is estimated at 5–8 m and reached a climax shortly before or at the beginning of the eruption (see Dvorak and Gasparini, 1991; Dvorak and Mastrolorenzo, 1991). The ground surface started to sink again after the eruption. Quantitative measurements of ground sinking began in 19th century, when Niccolini (1845) periodically measured the depth of the floor of a Roman market (Serapeo) covered by seawater. The first topographic leveling survey was carried out in 1905. Further leveling surveys were carried out in 1919, 1922, 1953 and 1968. All these data indicated a rather continuous sinking with an average rate of 1.3 cm/year (Berrino et al., 1984). Since 1970 two uplift episodes inverted the previous trend: the first one occurred from 1970 to 1972, the second one from 1982 to 1984. The maximum uplift from 1970 to 1972 was of about 1.50 m and was followed by a sinking recovering about 14% of the uplift. The 1982–1984 episode had a maximum uplift of about 1.80 m, followed by a sinking which up to now has recovered more than 30% of the uplift. The inflating and deflating areas appear to have a circular symmetry of about 6 km radius with no significant differences of shape and size between inflating and deflating episodes (Avallone et al., 1999). Low magnitude seismic activity ( $M_l = 1-4$ ) was moderate during the 1970–1972 inflation episode and very intense during the 1982–1984 episode. The latter was concentrated at depths shallower than 3 km (Aster et al., 1992) in the zone of higher uplift gradient (Berrino and Gasparini, 1995). The possible occurrence of a magma reservoir at about 4 km of depth is indicated by the identification of a P-SV converted phase in a seismic profile (Ferrucci et al., 1992), by the maximum depth of earthquakes (Aster et al., 1992; De Natale and Pingue, 1993) and by petrological and geochemical data (see Armienti et al., 1983; Civetta et al., 1991).

The first genetic models of the ground deformation pattern ascribed it to a pressure increase at the top of a shallow magma chamber embedded in an elastic medium (Yokoyama, 1970; Berrino et al., 1984; Bonasia et al., 1984; Bianchi et al., 1984–1987; Dragoni and Magnanensi, 1989; Dvorak and Berrino, 1991, De Natale and Pingue, 1993;). DInSAR images collected in the period 1993 to 1996 have a very dense space coverage and allow a reliable estimate of the Mogi-type pressure source location. It has been located about 800 m offshore SW of the town of Pozzuoli at a depth of about 2700 m (Avallone et al., 1999). Bonafede et al. (1986) considered the pressure source embedded in a viscoelastic medium, while Como and Lembo (1992) developed a numerical model to simulate the effects of fracturation and conductive thermal propagation on the ground deformation. All these models require overpressures of several hundreds MPa to justify about 3 m of maximum ground uplift in an elastic medium. If a viscoelastic medium is assumed, an unrealistic viscosity as low as 1016 Pas is necessary in order to keep the overpressure within reasonable values (Troise, 1999). Finally, the sudden deflation of the area without the occurrence of any eruption cannot be easily explained with mechanical source models.

Oliveri del Castillo and his coworkers were the first to propose that the fast inflation and deflation of the Campi Flegrei caldera could have been an effect of variation of pore pressure related to the temperature of fluids in permeable rocks (Oliveri and Quagliariello, 1969;

Casertano et al., 1976). Bonafede (1991) and De Natale et al. (1991) showed in more detail how the heating of groundwater in permeable rocks can produce the overpressures needed to cause the observed ground deformation. 1D and 2D numerical models based on the application of non equilibrium thermodynamics to the interaction between a thermal source and the circulation of groundwater in a permeable system (Ascolese et al., 1993; Gaeta et al., 1997) have shown that hydrothermal systems have the effect of amplifying the ground deformation. In fact they transmit to shallower depth and on larger surfaces the increase of pressure occurring at the base of the layer. Therefore the motion of the front of overpressure should cause a progressive transfer to shallower depths of the inflation centre. However, this phenomenon has not been detected by any of the geophysical measurements in the area. De Natale et al. (1997) argue that this is due to the caldera walls acting as rigid boundaries which make the shape of the surface deformation area rather insensitive to the depth of overpressure source. Recently Wohletz et al. (1999) and Orsi et al. (1999), performed finite elements numerical simulations accounting for conductive and convective heat transfer and a variety of sizes of magma reservoirs. They conclude that the contribution of convective heat transfer is needed to justify the temperature variations with depth observed in several geothermal wells.

In order to validate thermal and mechanical numerical models it is necessary to have a complete overall picture of the thermal regime existing in the upper 4 km of the Campi Flegrei caldera and the elastic/anelastic rock properties. The present models are tested against the temperature profiles measured in deep geothermal wells drilled in two sites inside the caldera (S.Vito and Mofete) (AGIP, 1987). The measured temperatures indicate that the inner part of the caldera is actually the site of significant thermal anomaly (a temperature of 420 °C was measured at 3 km of depth at the S.Vito 1 well). Consistently, surface geothermal gradients of about 150–200 °C/km are measured in the AGIP deep wells and in shallow boreholes inside the caldera (Corrado et al., 1998).

The study of attenuation of seismic waves can integrate these spotty and shallow data and provide an overall picture of the thermal regime in the upper 3 km of crust inside the Campi Flegrei caldera. In fact, laboratory measurements in the seismic frequency range (Kampfmann and Berckemer, 1985) indicate an exponential Arrhenius-law type increase of intrinsic attenuation with the temperature of the rocks. Several recent works in geothermal areas (Zucca et al., 1994; Sanders and Nixon, 1995; Sanders et al., 1995; Wu and Lees, 1996) have shown that the imaging of the quality factor  $Q$  is a useful tool to define location and extension of magma bodies in volcanic areas and to detail the fluid contribution through fractured systems. Usually, high-degree of cracking or high effective porosity (Zucca et al., 1994 Sanders et al., 1995) and the presence of water/gas in the fractures lower both  $P$  and  $S$  wave quality factors  $Q_p$  and  $Q_s$ .

At a global scale, a high degree of correlation is found between high heat-flow and low- $Q$  zones (Sato and Sacks, 1989; Mitchell, 1995; Romanowicz, 1995), despite the uncertainties in comparing estimates of  $Q$  from different methodologies (Romanowicz, 1998) and in discerning the contributions of effective porosity and temperature (Liu et al., 1994).

The availability of a high quality set of 3 component digital recordings obtained during the 1982–1984 seismic crisis allows to improve our knowledge of the thermal state of the caldera by performing a tomographic inversion of the intrinsic attenuation of  $P$ -waves. The existence of deep geothermal wells (up to 3 km of depth) enables us to constrain the obtained thermal model with in situ measured temperatures.

The aim of this paper is to present the results of the 3D  $Qp$  imaging, to discuss the local  $Qp$ – $T$  conversion and to infer the thermal properties of the deep part of the caldera.

## 2. Data

The data considered in this study represent a high-quality subset of 87 events belonging to a microearthquake set recorded from January till June 1984 by a local seismic network consisting of 12 three-component digital (12 bit) seismographs, installed in the framework of a cooperative project between University of Wisconsin and Osservatorio Vesuviano (Aster et al., 1992). On each  $P$  direct phase we measured the rise time (the time lag between the arrival time of the signal and the first zero crossing time, i.e. half a period) and pulse width  $\Delta T$  (the time lag between the arrival time of the signal and the second zero crossing time, i.e. a complete period). The number of data for each of the selected events range from a minimum of 8 to a maximum of 18, depending on the number of recordings and on data quality. The ray coverage is shown in Fig. 1. The total number of pulse data for our analysis is around 1000 (Fig. 2). The 3D  $P$ -wave velocity structure inferred by Aster and Meyer (1988) was used to compute travel times. The short distances traveled by the waves (from 3 to 10 km) justify the assumption of a straight line ray-propagation.

## 3. The inversion method

Source parameters and quality factor were computed using the method proposed by Zollo and de Lorenzo (in press). This is a version of the classical “rise time method” (Gladwin and Stacey, 1974) modified to account for the effects of finiteness of the seismic source and the consequent directivity often observed on waveforms generated by earthquakes. The method is based on the numerical solution of a set of non linear equations relating data (rise time and pulse width) to source (radius, dip and strike) and attenuation (3D distribution of  $Qp$ ). The fault is modeled as a Sato and Hirasawa (1973) (S&H) circular crack, and the attenuating medium is discretized in rectangular blocks.

The data space consists of the measurements of rise-times  $\tau_{i,j}$  and pulse widths  $\Delta T_{i,j}$  ( $i=1,\dots,N$ ;  $j=1,\dots,M_i$ ) of  $N$  microearthquakes recorded at a network of  $M$  receivers;  $M_i$  represents the number of receivers that recorded the  $i$ -th event.

The source parameters space, for each event, consists of:

- the radius  $\rho_{0,i}$  of the S&H circular crack (we assume a fixed, known value for rupture velocity)
- the dip and the strike  $\phi_i$  of the fault plane.

As the travel time  $T_i$  in the  $i$ -th block is evaluated from the velocity model, the attenuation parameters space consists of the quality factors  $Q_i$  of each block crossed by the  $P$ -ray. Therefore, the global attenuation term  $T/Q$  is:

$$\frac{T}{Q} = \sum_{i=1}^P \frac{T_i}{Q_i}$$

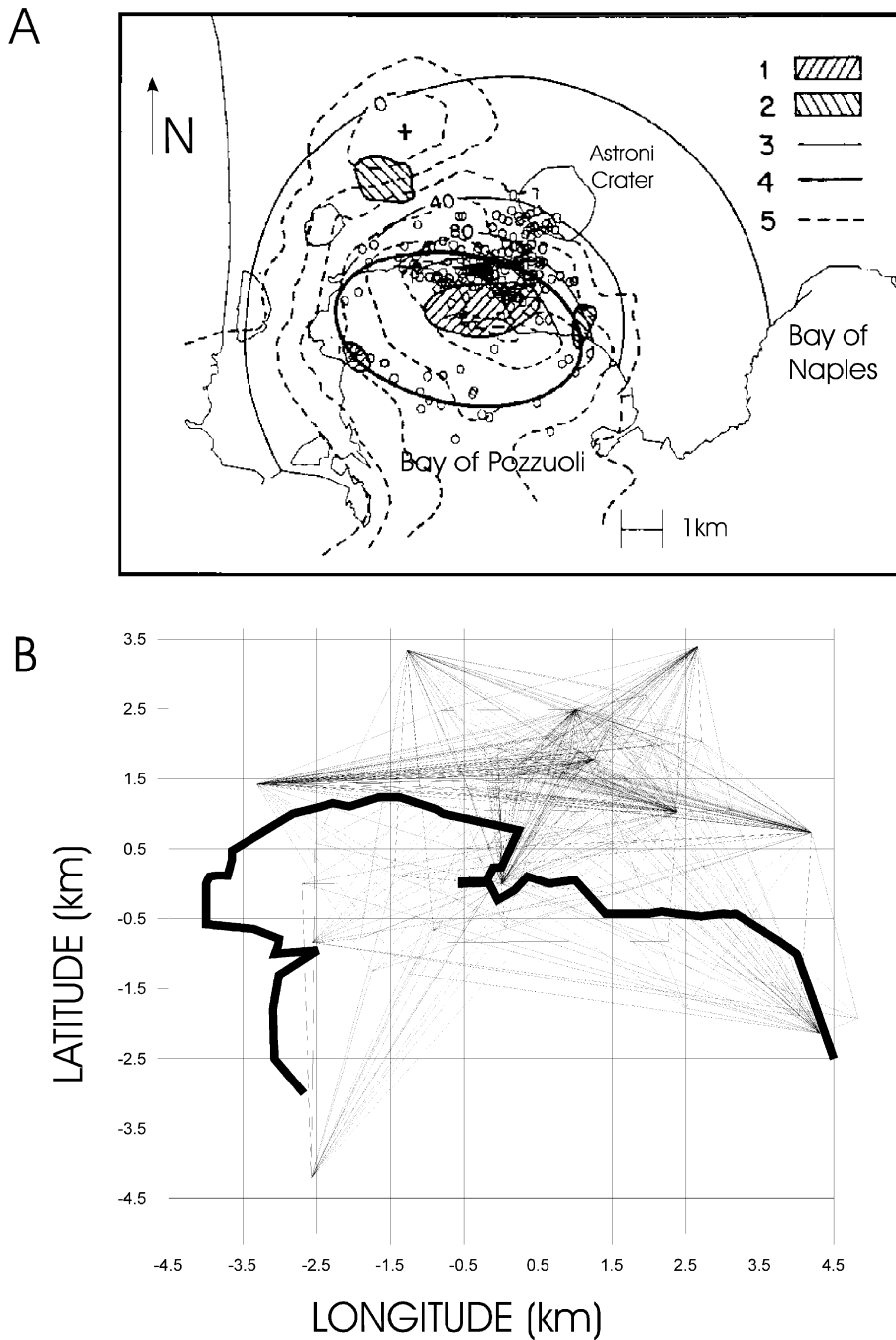


Fig. 1. (A) Earthquake epicenters (February–June 1984) with other geophysical results superimposed: 1. areas of  $V_p/V_s > 1.9$  at 1 km depth; 2. areas of  $V_p/V_s < 1.6$  at 1 km depth; 3. 40-cm elevation contours for the 1982–1985 uplift (data from Osservatorio Vesuviano: Rapporto Sorveglianza 1985); 4. elliptical trace of the hypothesized ring fault of Aster and Meyer (1988); 5. 1 mgal Bouguer gravity contours (after Aster et al., 1992). (B) Horizontal ray coverage for the 87 earthquakes considered in this study.

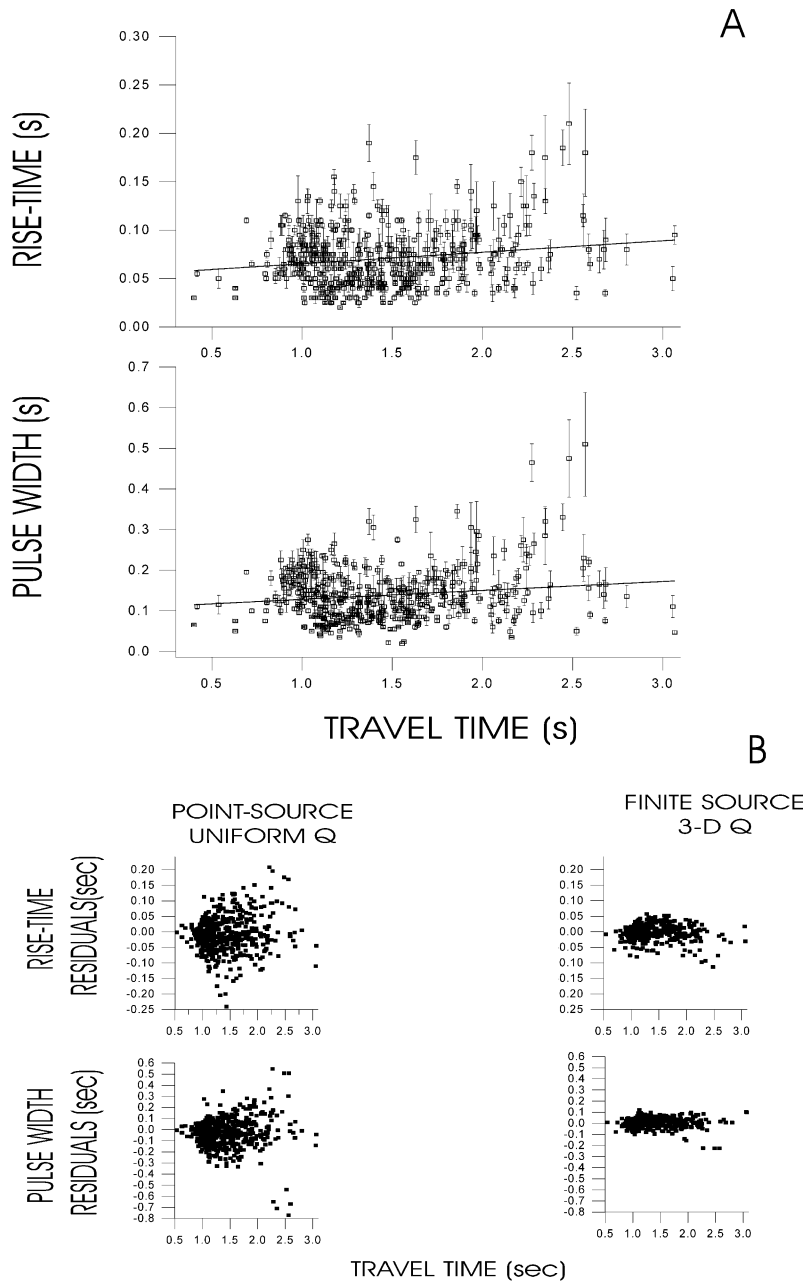


Fig. 2. (A) Pulse width and rise time vs. travel time of the analyzed data set. Also shown is the least squares straight line corresponding to the delta-like sources and homogeneous  $Q$  structure assumption. Note the large scattering of both data sets around the best fitting straight line. This may be due both to the source effects and/or to the heterogeneity of the attenuation parameters of the crust at the Campi Flegrei caldera. (B) Residuals between rise time (and pulse width) data and the corresponding “data” predicted by the model as a function of the travel time. On the left are shown the residuals corresponding to the assumption of a point-like source and homogenous  $Q$  model, on the right those corresponding to the assumption of a finite dimension seismic source and the 3D attenuation structure.

The source and attenuation model space consists of  $3N + P$  parameters. The non linear system of equations to be solved is therefore given by (Zollo and de Lorenzo, in press):

$$\tau_{i,j} = \frac{\rho_{0,i}}{v_R} - \frac{\rho_{0,i}}{c} \sin \Omega(\delta_i, \phi_i) + \gamma_{i,j} \sum_{m=1}^P \frac{T_{i,j,m}}{Q_m} + \lambda_{i,j} \quad 1 \leq i \leq N \quad (1)$$

$$\Delta T_{i,j} = \frac{\rho_{0,i}}{v_R} + \frac{\rho_{0,i}}{c} \sin \Omega(\delta_i, \phi_i) + 3.9 \sum_{m=1}^P \frac{T_{i,j,m}}{Q_m} \quad 1 \leq j \leq M_i$$

$$\gamma_{i,j}(\rho_{0,i}, c, \theta) = \gamma_1 \frac{\rho_{0,i}}{c} \sin \Omega(\delta_i, \phi_i) + \gamma_2 \quad (2)$$

$$\lambda_{i,j}(\rho_{0,i}, c, \theta) = \lambda_1 \frac{\rho_{0,i}}{c} \sin \Omega(\delta_i, \phi_i) + \lambda_2 \quad (3)$$

where:

$$\begin{aligned} \gamma_1 &= 6.601 \pm 0.015 \\ \gamma_2 &= 0.946 \pm 0.015 \\ \lambda_1 &= 0.051 \pm 0.015 \\ \lambda_2 &= -0.005 \pm 0.015 \end{aligned} \quad (4)$$

In  $Q_s$ . (1)–(4)  $c$  represents the phase velocity of  $P$  waves,  $v_R$  is the rupture velocity,  $T_{i,j,m}$  represents the travel time of the first  $P$ -wave generated by the  $i$ -th event recorded at  $j$ -th station passing through the  $m$ -th block, and the take-off angle  $\Omega(\delta_i, \phi_i)$  between the  $i$ -th source and the  $j$ -th receiver is given by:

$$\Omega(\delta_i, \phi_i) = \arccos \left\{ \frac{R_{i,j}^2 + 1 - T_{i,j}^2}{2R_{i,j}} \right\}$$

The search for the best fit model parameters is performed through a two-step procedure (fixed source parameters, inversion of  $QP$ ; fixed  $QP$  structure, inversion of source parameters) based on the search of the minimum weighted  $L^2$  norm.

The exploration of the parameters space is realized throughout the “Downhill Simplex method” (Nelder and Mead, 1965; Press et al., 1994) with initial completely random model. The robustness and efficiency of the inversion method has been investigated through synthetic simulations with noised computed data, as detailed in Zollo and de Lorenzo (in press). In particular, for Campi Flegrei data, the reliability of the retrieved source and attenuation models is quantitatively assessed by ad hoc resolution tests and error mapping (Zollo and de Lorenzo, in press).

#### 4. Inversion of Campi Flegrei microearthquake data: *P*-wave attenuation images and their resolution

In this paper we deal with the computed attenuation parameters while the results of the inversion concerning the estimate of source parameters are discussed by de Lorenzo et al. (in press). Although the *P*-wave travel distances are rather short, both rise time and pulse width data show a dependence on travel time, even if with a large scatter (Fig. 2). At the microearthquake scale both shape and frequency content of seismograms can be affected by source directivity (Zollo and de Lorenzo, in press).

The application of the classical rise time method (Wu and Lees, 1996) under the assumption of homogenous  $Q_p$  structure produces average residuals of 0.053 s for rise time and of 0.121 s for the total pulse width. The residuals as a function of the travel time are shown in Fig. 2.

The application of the Zollo and de Lorenzo's (in press) method under the same assumptions reduces to half the variance both of rise time and pulse width residuals with respect to the case of a point-like impulsive source. The  $Q_p$  value obtained from the inversion of all the data in the assumption of a homogeneous attenuating medium is  $Q_p = 280 \pm 70$ . However, the apparent  $Q_p$  values for each source-receiver configuration (i.e. the best fit value for each considered event) range from  $Q_p = 18$  to  $Q_p = 862$ . This large  $Q_p$  variability per event is a clear indication of the high heterogeneity of the attenuation structure.

The uncertainty of  $Q_p$  images has been estimated using the approach followed by Vasco and Johnson (1998). It consists in mapping random deviations of data in the model parameters space. Errors on  $Q_p$  range from 10 to 30% of the estimated value (de Lorenzo et al., in press)

A significant reduction of residuals is obtained if a finite source and a 3-D space variation of  $Q$  are considered (Fig. 2b). The final value of the variance was  $1.30 \text{ s}^2$  (corresponding to a r.m.s. = 0.037 s). The present finite source and 3-D attenuation model provides a global variance reduction of 38% with respect to the finite source and homogeneous  $Q_p$  model (Fig. 2).

The resolution of 3-D dimensional images has been investigated using fixed geometry and checkerboard tests (Zollo and de Lorenzo, in press). The fixed geometry tests are aimed at defining the reliability of the recovered shapes and the amplitudes of specific attenuating bodies. The checkerboard test provides a quantitative estimate of space parameters correlation and of the resolved wavelength. In this study only the checkerboard test is described. It consists of imaging a synthetic  $Q_p$  structure formed by an alternation of low ( $Q = 50$ ) and high  $Q$  ( $Q = 600$ ) blocks (Fig. 3). This test indicates that a higher resolution is expected in the central part of the caldera at middle depths (1–2 km). At shallow depths (less than 1 km) a highly resolved image is obtained for the whole region with the exception of the peripheral blocks. At large depths (2–3 km) the image is less resolved and only to the central region appears rather well constrained.

The loss of resolution with depth is a combined effect of the increasing *P*-wave travel distances and of the smaller ray sampling for deep blocks. We infer that the western part of the caldera is not resolved by the considered data set at depths greater than 2 km.

##### 4.1. Main features of the obtained 3D $Q_p$ maps

The main features which can be observed from the tomographic 3D  $Q_p$  images are (Fig. 4):

TRUE Q STRUCTURE

RECOVERED Q STRUCTURE

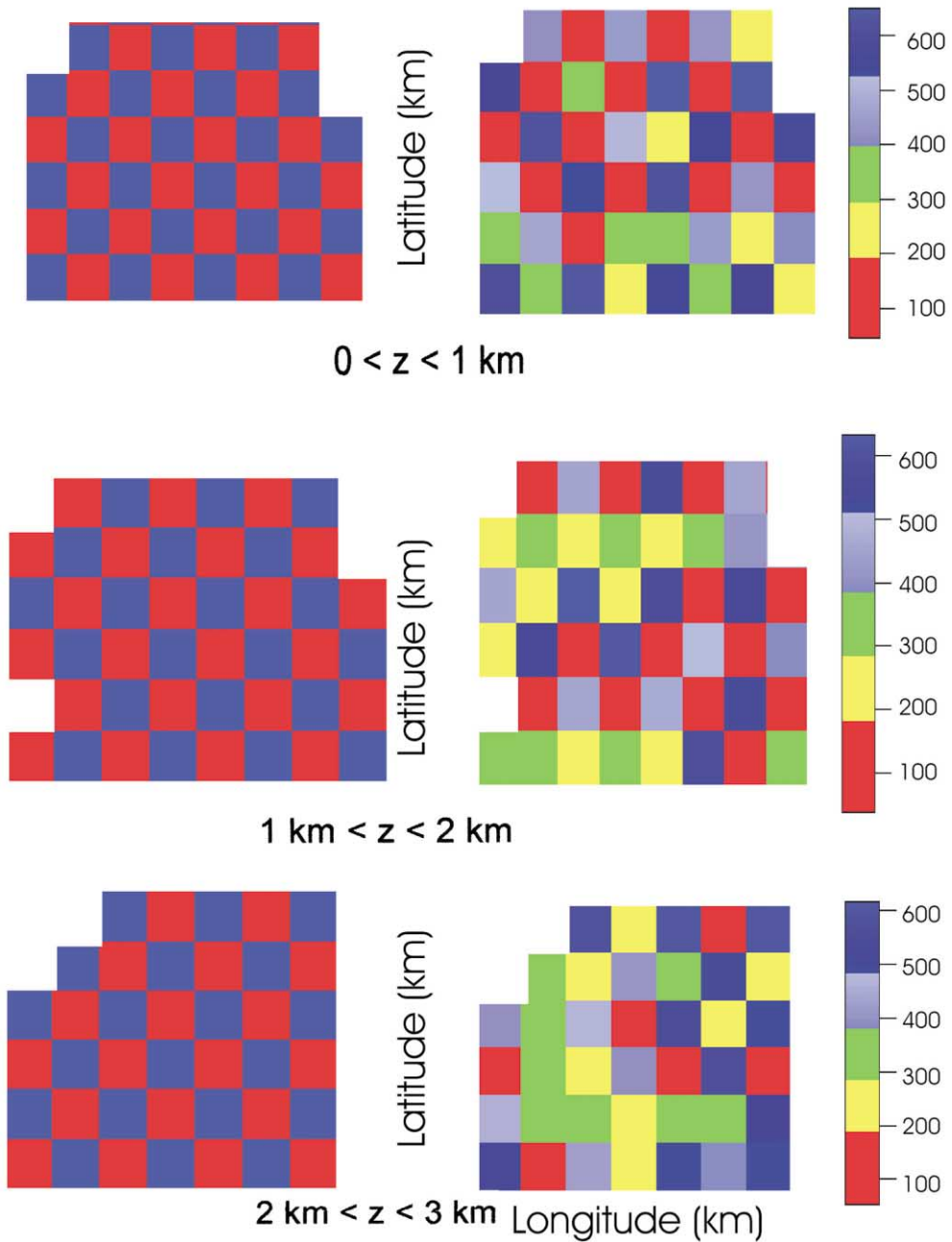


Fig. 3. Checkerboard resolution test for the three dimensional case. On the left is shown the true attenuation structure (low  $Q=100$ , high  $Q=600$ ), on the right the recovered  $Q$  structure.

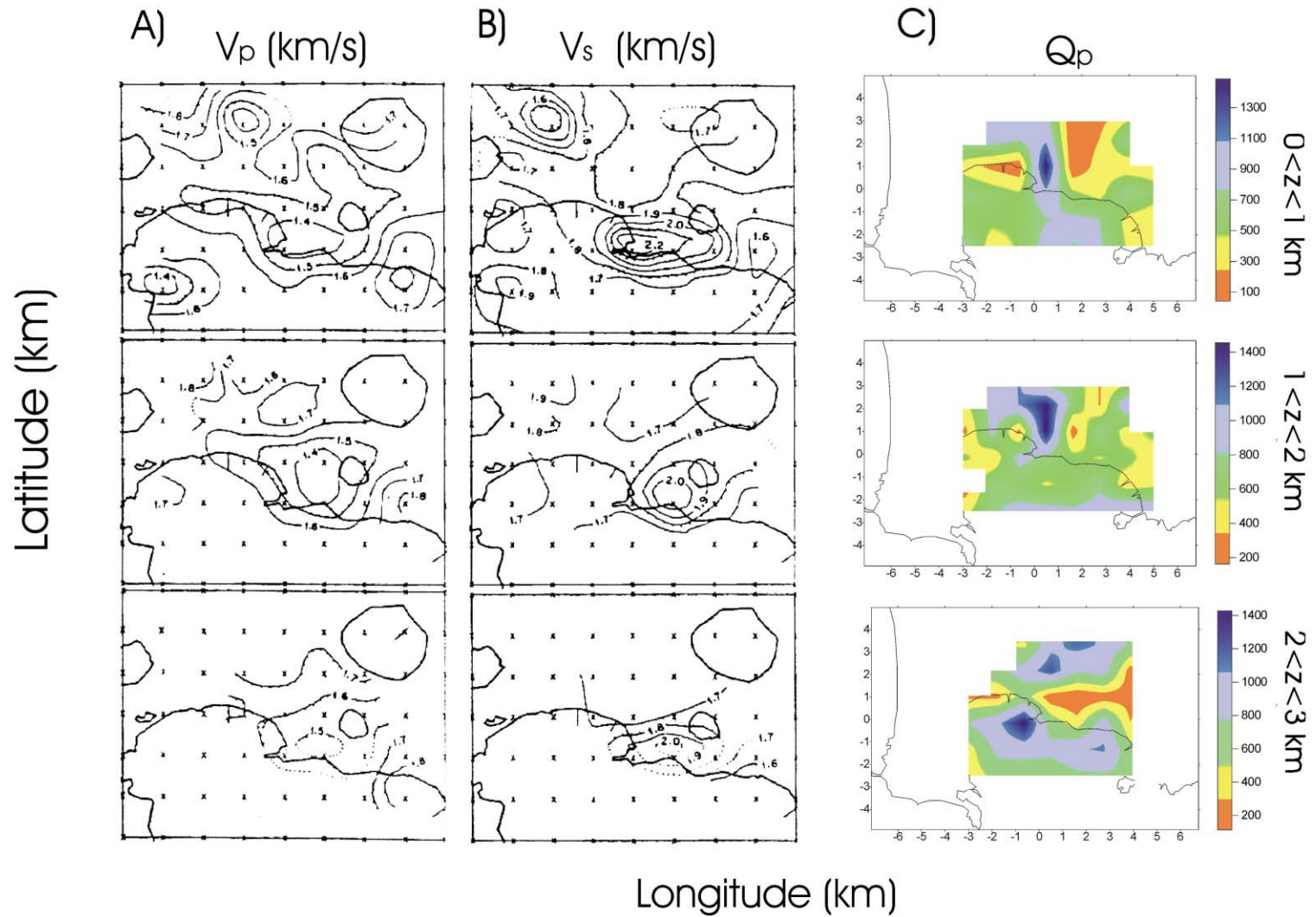


Fig. 4. (A) Three-dimensional  $V_s$  map at the Campi Flegrei caldera (after Aster and Meyer, 1988). (B) Three-dimensional  $V_p/V_s$  map at the Campi Flegrei caldera (after Aster and Meyer, 1988). (C) Three dimensional  $Q_p$  attenuation structure of the Campi Flegrei caldera.

- the shallow layer (from 0 to 1 km depth, in the following referred to as layer 1) is characterized by a central N–S elongated high  $Q_p$  anomaly. It separates two low  $Q_p$  areas, one centered NE of the town of Pozzuoli, the other in the Solfatara-Agnano area;
- the same trend with smoother lateral variations of  $Q_p$  occurs in the intermediate layer (between 1 and 2 km depth, in the following referred to as layer 2) with extremely localized low- $Q_p$  values.
- in the layer between 2 and 3 km depth (layer 3) the trend changes. An east–west trending low  $Q_p$  anomaly, located in the central-eastern part of the caldera, is the most prominent feature.

$Q_p$  tomographic images correlate well with seismic wave velocity maps inferred by first arrival time inversion (Aster and Meyer, 1988) (Fig. 4). The low- $Q_p$  region of layer 3 matches well both location and geometry of the low- $V_s$  region and high  $V_p/V_s$ .  $V_p/V_s$  is about 1.9 at 3 km depth, and it increases to 2.2 toward the surface (layer 1). The correlation between  $Q_p$  and  $V_s$  appears weaker moving to shallower depths, although high  $V_s$  are located on the N edge of the high  $Q_p$  anomaly in layers 1 and 2. Aster and Meyer (1988) attributed the high  $V_p/V_s$  value at shallow depths to the effect of fluid-filled cracked rock materials. The decrease of  $V_p/V_s$  with depth and the correlation between low- $Q_p$  and low- $V_s$  in layer 3 suggest that thermal effects are dominant in this region.

#### 4.2. Comparison with previous attenuation measurements in the area

Previous  $Q$  determinations at the Campi Flegrei were based on the modeling of the spectral properties of coda waves and direct S waves. It was shown that coda  $Q$  ( $Q_c$ ) is almost independent on frequency (Del Pezzo et al., 1987; Aster et al., 1992). This effect was interpreted as evidence that intrinsic attenuation is dominant over scattering attenuation. This seems to be a characteristic of volcanic areas where intrinsic attenuation should be strongly affected by the high temperature fields produced by melting or intruded hot bodies.

De Natale et al. (1987) determined an average value of direct S wave quality factor in the area ( $Q_s = 110 \pm 50$ ) by using a spectral technique. Considering the average  $Q_p$  value obtained in the present study ( $Q_p = 280 \pm 70$ ) we obtain that  $Q_p/Q_s = 2.6$ . Regional (Sato and Sacks, 1989) and laboratory (Kampfmann and Berckemer, 1985)  $Q$  determinations coherently indicate that  $Q_p/Q_s \approx 2.2$ – $2.6$  when the energy is primarily dissipated by shear deformation.

Our results are also consistent with the kappa ( $\kappa = T/Q$ ) parameter of Anderson and Hough's (1984) attenuation model estimated from acceleration spectra at the Campi Flegrei caldera (De Natale et al., 1987):  $\kappa = 0.015 \pm 0.02$  s for SH waves and  $0.008 \pm 0.0027$  s for  $P$  waves. Assuming a mean  $P$ -wave travel distance of 7 km and  $V_p = 3$  km/s an equivalent  $Q_p = R/(v \kappa) \approx 90$  is obtained.

### 5. Inferences on the thermal structure of the Campi Flegrei Caldera

The quality factor is actually considered as the seismological parameter more strictly dependent on the thermal properties of the rocks (e.g. Mitchell, 1995; Sato and Sacks, 1989). Several laboratory measurements indicate an exponential dependence of  $Q$  on the inverse of the absolute

temperature (Arrhenius law). As argued by Romanowicz (1998) the non linear sensitivity of  $Q$  to temperature implies that attenuation tomography should be able to resolve hot regions (high attenuation) better than elastic tomography. Kampfmann and Berckemer (1985) determined the parameters of the exponential dependence of  $Q$  on temperature by laboratory measurements on rock materials undergoing forced oscillation in the range 0.03–30 Hz. For  $Q_p/Q_s$  in the range 2.2–2.6, they found:

$$F = 1160 - 150 \log Q_p \tag{6}$$

where  $F$  is temperature in degrees.

Moreover, they observed that, for temperatures lower than 900 °C, the above equation holds for any materials irrespective of its chemical composition. Wu and Lees (1996) imaged the temperature field at depth in the Coso (California) geothermal area by converting  $Q$  to through Eq. (6). Actually, the main problem in recovering  $F(Q_p)$  is the need to discriminate the thermal effect from effects due to variations of permeability. This problem is relevant in volcanic areas characterized by intensive geothermal activity. Both laboratory and seismological studies (see e.g. Sanders et al., 1995 and references therein; Zucca et al., 1994) have in fact shown that  $Q_p$  and  $Q_s$  strongly decrease with increasing permeability and fluid circulation in cracked rocks.

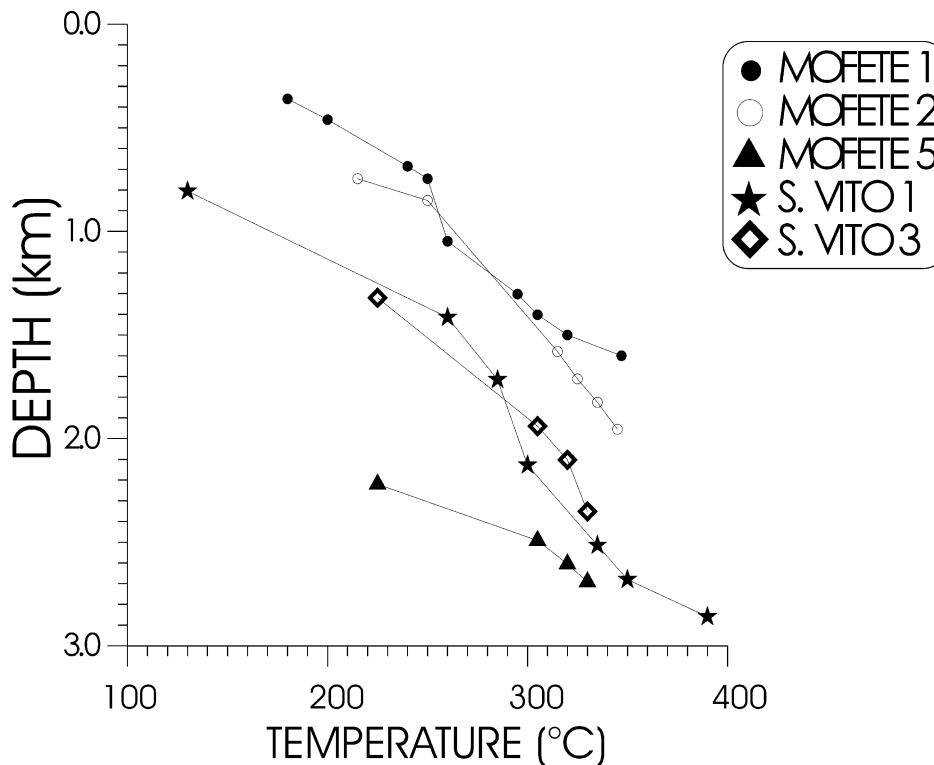


Fig. 5. Temperature measurements as a function of the depth in five AGIP geothermal wells.

Because of this ambiguity and of the possible dependence of  $Q$  on frequency, Sato and Sacks (1989) pointed out the need of calibrating ( $Qp$ ) measurements using local thermal data.

Our knowledge of the thermal state of Campi Flegrei arises both from temperature measurements in five deep AGIP boreholes (Fig. 5) (AGIP, 1987) and from thermal measurements in thirty-seven surface boreholes (up to 140 m of depth) (Corrado et al., 1998; Fig. 6). The geothermal surface gradient map compiled by Corrado et al. (1998) provides clear evidence for strong lateral variation of the geothermal gradient due to the effect of groundwater motion through the surface aquifers. After removal of thermal disturbances due to the water flow, Corrado et al. (1998) estimated an average geothermal gradient in the range 150–200 °C/km.

The residual geothermal gradient map, obtained by subtracting the average geothermal gradient from the unfiltered field, enhances small wavelength highs located at Mofete, north of M. Nuovo and at the Agnano crater (Fig. 6). AGIP MF1 and MF2 deep wells are located on the top of the Mofete anomaly and MF5 is located on its N edge. In contrast, the San Vito wells (SV1 and SV3) are located in an area where no local thermal anomaly is present.

Temperature and hydrothermal mineral zonation  $V$ s depth furnish consistent information on the geothermal system existing at the Campi Flegrei caldera. A mineral zonation typical of hydrothermal systems is well developed in the Mofete wells and, although less clear, in the San Vito wells (Chelini and Sbrana, 1987). Argillitic and illite-chlorite paragenesis are ubiquitous

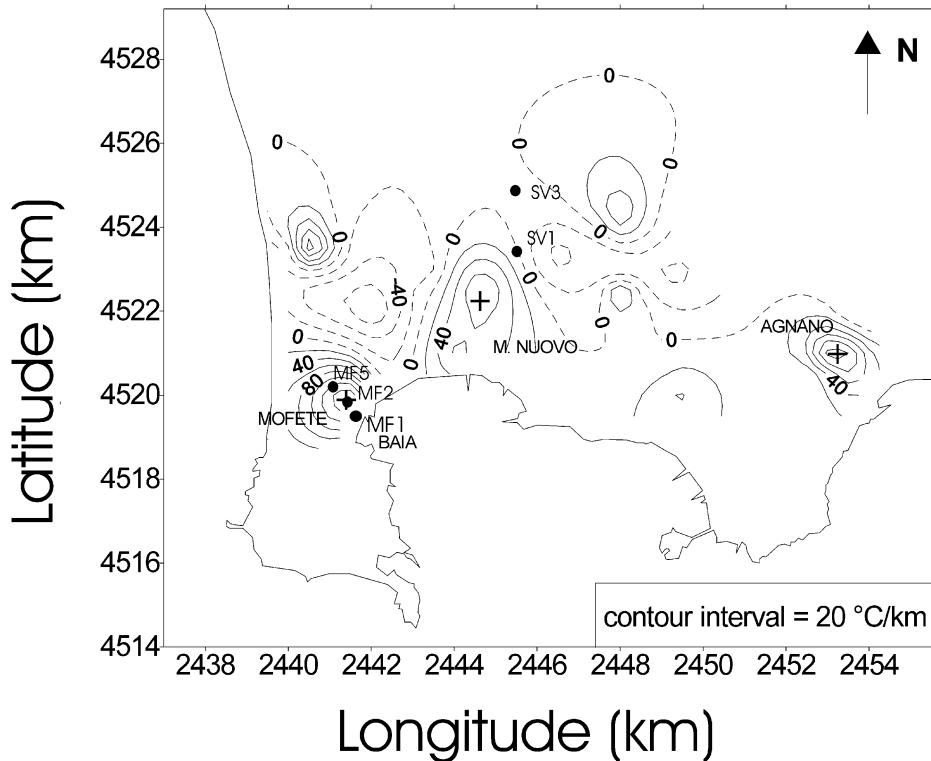


Fig. 6. High pass filtered map of the surface geothermal gradient at the Campi Flegrei caldera (after Corrado et al., 1998).

down to a depth of 750–900 m (MF1 and 2), of 1400 m (MF5) in the Mofete area and down to 1400 m (SV3)–1750 m (SV1) in the San Vito area. They are due to mineral transformations at temperatures lower than about 250 °C. The produced rock has a very low permeability and forms the impervious cap rock of the geothermal system. At greater depth neogenic minerals (K-feldspar, adularia, albite, quartz) are dominant. They are formed by precipitation from hot water cooled by the contact with the host rocks. This zone (calc-aluminum silicate zone) defines the top of the circulating fluid system. The resulting rock is often highly permeable. The temperatures measured in the wells at the depth corresponding to the transition from the illite-chlorite to the calc-aluminum silicate zone are 250 °C at Mofete and 220–270 °C at San Vito.

The temperature gradients measured and inferred in wells MF2 and MF5 are much higher than those in boreholes SV1 and SV3, consistent with the average values observed in shallow wells. MF wells have met important aquifers running on the argillitic zone (150–300 m of depth) and within the calc-aluminum silicate zone (1250–1600 m of depth) and also at greater depth. No evidence for widespread aquifers was found at the SV wells, except for a very shallow water table in the yellow tuff and pyroclastics.

This confirms that the present fluid circulation scarcely affects the geotherms of boreholes SV1 and SV3, which can be assumed to represent mostly a little-disturbed conductive gradient typical of the area. These geotherms show a mean gradient of 130–210 °C/km at depths smaller than 1.5 km and of 44–64 °C/km at greater depths. This abrupt change may be explained by a change of the thermal conductivity, from typical surficial tuffs values (0.85 W/mK) (Corrado et al., 1998) to higher values expected for high temperature hydrothermal altered rocks (2–3 W/mK).

In order to establish a  $VQ_p$  calibration curve for Campi Flegrei we considered the values of  $Q_p$  obtained by tomographic inversion between 1 and 3 km at the blocks near wells SV1 and SV3 and we correlated them to the temperatures observed at the same depths. This analysis provided the following empirical equation:

$$F = 713 - 61 \log(Q_p) \quad (7)$$

The standard deviation of  $Q_p$  and the temperature ranges are also shown in Fig. 7, where the K&B relation (Eq. 6) is shown for comparison. The shaded area represents the accuracy of  $Q_p$ . The values of  $\ln(Q_p)$  obtained by Eq. (7) are higher than those obtained by the K&B equation in the range of values inferred at Campi Flegrei. This may be due to the effect of lithostatic pressure which contributes to the increase of  $Q_p$ . If this is the case, it is possible to evaluate the rate of change of  $\log(Q_p)$  with pressure. In fact, this effect may be roughly expressed by:

$$\alpha = \frac{\partial \log(Q_p)}{\partial P} \quad (8)$$

If an average density of 2300 kg m<sup>-3</sup> is assumed,  $\alpha$  is 9.0<sup>-9</sup>

The temperature maps at depths between 1–2 and 2–3 km as inferred by the  $Q_p$  estimates using Eq. (7) are reported in Fig. 8. A positive thermal ( $Q_p$ ) anomaly can be seen East of the Mofete area, in agreement with temperatures measured in wells. However, the details of this anomaly must be considered with caution because: (1) the resolution in this area is poor, as shown in Fig. 3,

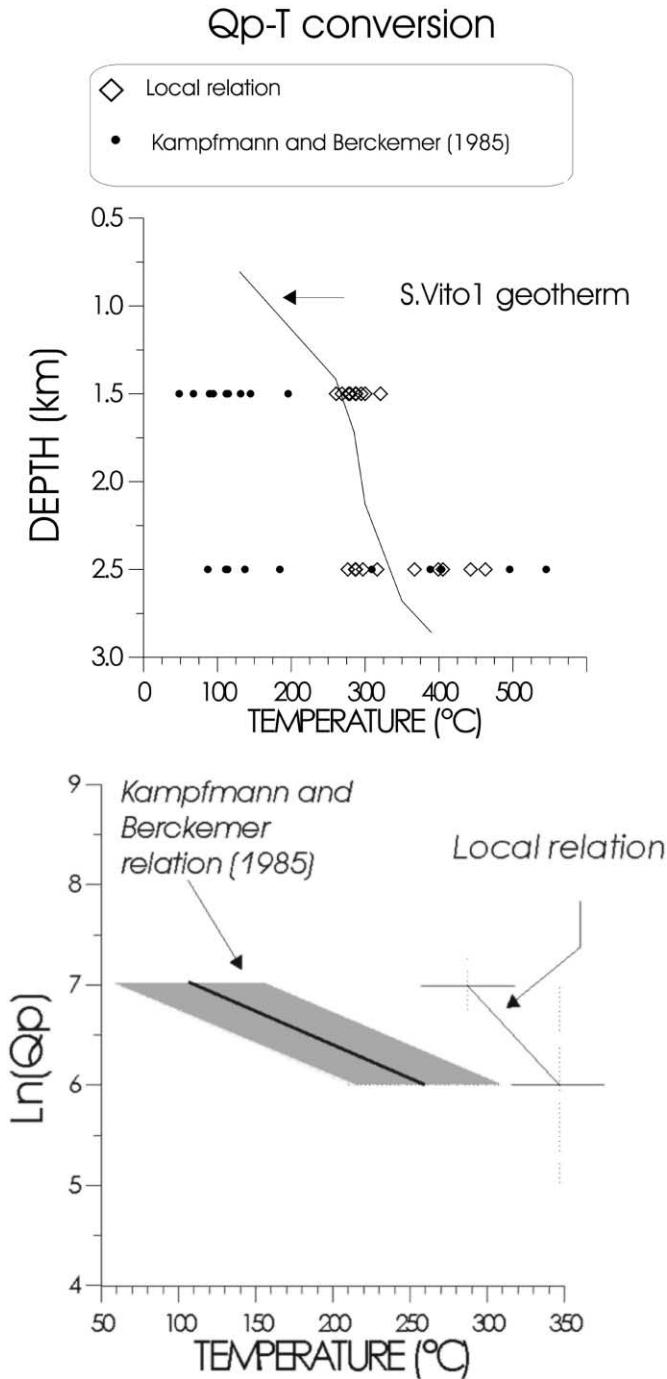


Fig. 7. (A) Comparison between ( $Qp$ ) estimated by the Kampfmann and Berckemer (1985) relationship and ( $Qp$ ) values inferred by the calibration procedure described in the text. Also it is shown the geotherm of the SV1 geothermal well. (B) Comparison between the Kampfmann and Berckemer (1985) relationship and the  $F = (Qp)$  curve inferred by the local calibration.

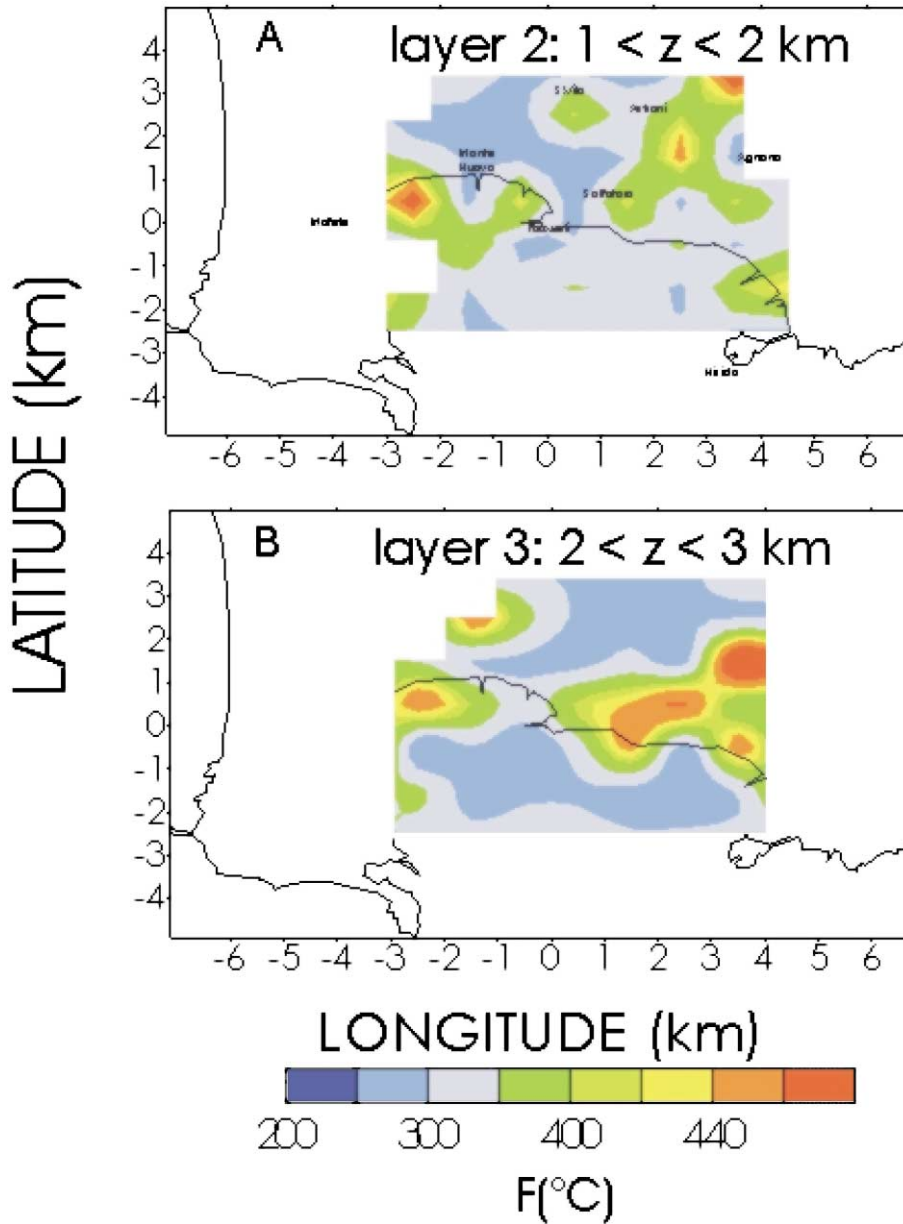


Fig. 8. (A) Temperature map at depth between 1 and 2 km as inferred by the local  $Q_p$ -conversion. (B) Temperature map at depth between 2 and 3 km as inferred by the local  $Q_p$ -conversion.

(2) the temperature dependence of  $Q_p$  cannot be separated from the effects due to the important thick aquifers found deeper than 1 km.

The most significant low  $Q$ , high anomaly at depths greater than 2 km extends eastward of the town of Pozzuoli, encompassing an area that includes the craters of Astroni, Agnano (where a high thermal gradient was measured, see Fig. 6) and Solfatara. Many recent eruptions occurred in

this area and present hydrothermal phenomena (hot waters, fumaroles) are here concentrated. The location and geometry of this anomaly correlate well with the EW elongated region of low- $V_s$  observed by local earthquake tomography (Aster and Meyer, 1988) (Fig. 4).

Several lines of evidence suggest the presence of a local magma reservoir at shallow depths. Bianchi et al., (1987) and Ferrucci et al. (1992) suggested a top of a hypothetical magma chamber at about 4 km depth on the basis of deformation and active seismic data. Wohletz et al. (1999) estimated that the chamber had minimal volumes of 1000 and 160 km<sup>3</sup> before the Campania ignimbrite and the Neapolitan yellow tuff eruptions, respectively.

## 6. Conclusions

In this paper we have presented the  $Q$  attenuation structure arising from the joint inversion of rise time and pulse width data of direct  $P$  waves. The present thermal state of the caldera was inferred by calibrating  $Qp$   $V_s$  using temperature  $V_s$  depth curves of shallow and deep boreholes.

The  $Qp$  tomographic images clearly indicate a change of the anomaly pattern from the shallow/medium layers (1 and 2) to the deep layer (3). The shallow/medium depth region is characterized by a nearly  $N$  trending high  $Q$  anomaly which separates areas of rather low  $Q$ . The latter are located near the areas of Mofete and Agnano, where deep drilling has met hot fluid.

Instead, a major east–west trending, low  $Q$  anomaly is the dominant feature of the deepest layer. This region lies inside the inner caldera where the recent (since 11 kyear B.P.) magmatic activity has been concentrated (Barberi et al., 1991; Orsi et al., 1996) and where intensive hydrothermal activity is presently observed.

Seismic velocity estimates of Aster and Meyer (1988) indicate an anomalous high  $V_p/V_s$  ratio (2.2) at 0–1 km depth in the area where the eastern, low  $Q$  anomaly is located in the present study. This confirms that the dominant attenuation effect in this layer can be attributed to a fluid saturated volume.

At larger depths,  $P$ -wave attenuation and shear wave velocity anomalies have similar shape and extension, whereas the  $V_p$ -to- $V_s$  ratio decreases, reaching a value of 1.9–2.0 in layer 3. A similar pattern of decreasing values with depth is shown by porosity and transmissivity measured in the central caldera boreholes (De Vivo et al., 1989). All these lines of evidence suggest a dominant temperature, rather than fluid-filled crack effect on rock rheology for depths below about 2 km. Hence conduction can be considered as the dominant heat transfer mechanism in this depth range. This thermal anomaly can be the effect of a deeper heat source, as suggested by other geophysical and geochemical evidence.

## References

- AGIP, Geologia e Geofisica del sistema geotermico dei Campi Flegrei. DES, SERG-MESG, S. Donato, 1987.
- Anderson, J.G., Hough, S.E., 1984. A model for the shape of the Fourier amplitude spectrum at high frequencies. Bull. Seism. Soc. Am. 74, 1969–1993.
- Armienti, P., Barberi, F., Bizouard, H., Clocchiatti, R., Innocenti, F., Metrich, N., Rosi, M., Sbrana, A. 1983. Magma evolution within a shallow chamber: the Phlegraean Fields case. In: Sheridan M.F., Barberi F. (Eds.), Explosive Volcanisms (special issue). J. Volcanol. Geoth. Res. 17, 289–312.

- Ascolese, E., Aurisicchio, A., Briggs-Smith, M., Mita, D.G., Perna, G., Rossi, S., Gaeta, F.S., 1993. Thermodynamics of water-permeated unwelded pyroclasts, 2: non equilibrium properties. *J. Volcanol. Geoth. Res.* 57, 235–251.
- Aster, R., Meyer, R., 1988. Three-dimensional velocity structure and hypocenter distribution in the Campi Flegrei caldera, Italy. *Tectonophysics* 149, 195–218.
- Aster, R., Meyer, R., De Natale, G., Zollo, A., Martini, M., Del Pezzo, E., Scarpa, R., Iannaccone, G. 1992. Seismic investigation of the Campi Flegrei Caldera, in *Volcanic Seismology In: Proc. Volcanol. Series III*. Springer, New-York.
- Avallone, A., Zollo, A., Briole, P., Delacourt, C., Beauducel, F., 1999. Subsidence of Campi Flegrei (Italy) detected by SAR interferometry. *Geophys. Res. Lett.* 26, 2303–2306.
- Barberi, F., Cassano, E., La Torre, P., Sbrana, A., 1991. Structural evolution of Campi Flegrei caldera in light of volcanological and geophysical data. *J. Volcanol. Geoth. Res.* 48, 33–49.
- Berrino, G., Gasparini, P., 1995. Ground deformation and caldera unrest. *Cahier du centre Europ. Geodyn. Seismol* 8, 41–55.
- Berrino, G., Corrado, G., Luongo, G., Toro, B., 1984. Ground deformation and gravity changes accompanying the 1982 Pozzuoli uplift. *Bull. Volcanol.* 44, 187–200.
- Bianchi, R., Coradini, A., Federico, C., Giberti, G., Sartoris, G., Scandone, R., 1984. Modeling of surface ground deformations in the Phlegraean Fields volcanic area. *Bull. Volcanol.* 44 (14), 175–186.
- Bianchi, R., Coradini, A., Federico, C., Giberti, G., Lanciano, P., Pozzi, J.P., Sartoris, G., Scandone, R., 1987. Modeling of surface deformations in volcanic areas: the 1970–1972 and 1982–1984 crises at Campi Flegrei. *Italy J. Geophys. Res.* 92, 14139–14150.
- Bonafede, M., 1991. Hot fluid migration: an efficient source of ground deformation: application to the 1982–1985 crisis at Campi Flegrei–Italy. *J. Volcanol. Geoth. Res.* 48, 187–198.
- Bonafede, M., Dragoni, M., Quarenì, F., 1986. Displacement and stress fields produced by a center of dilatation and by a pressure source in a viscoelastic halfspace: application to the study of ground deformation and seismic activity at Campi Flegrei. *Italy Geophys J. R. Astron. Soc.* 87, 455–485.
- Bonasia, V., Pingue, F., Scarpa, R., 1984. A fluid filled fracture as a possible mechanism of ground deformation at Phlegraean Fields. *Italy Bull Volcanol* 47, 313–320.
- Casertano, L., Oliveri del Castillo, A., Quagliariello, M.T., 1976. Hydrodynamics and geodynamics in the Phlegraean Fields area of Italy. *Nature* 161, 141–154.
- Chelini W. Sbrana, A., 1987. Subsurface geology. In: *Phlegraean Fields Eds. Rosi, M., Sbrana, A. Quad. Ric. Sci.*, 114 (9), 175.
- Civetta, L., Carluccio, E., Innocenti, F., Sbrana, A., Taddeucci, G., 1991. Magma chamber evolution at Phlegraean Fields during the last 10 ka, in the light of trace elements and isotope composition. *European J. Mineral.*
- Civetta, L., Orsi, G., Pappalardo, L., Fisher, R.V., Heiken, G., Ort, M., 1997. Geochemical zoning, mingling, eruptive dynamics and depositional processes—the Campanian Ignimbrite, Campi Flegrei caldera, Italy. *J. Volcanol. Geoth. Res.* 75, 183–219.
- Como, M., Lembo, M., 1992. A thermo-mechanical model of the inflation and seismicity of volcanic calderas: an application to the Campi flegrei system, In: *Volcanic seismology Gasparini, P., Scarpa, R., Aki, K. (Ed.)*, pp. 547–568.
- Corrado, G., de Lorenzo, S., Mongelli, F., Tramacere, A., Zito, G., 1998. Surface heat flow density at Phlegraean Fields caldera. *southern Italy Geothermics* 27, 469–484.
- de Lorenzo, S., Zollo, A., Mongelli F., in press. Source parameters and 3-d attenuation structure from the inversion of microearthquake pulse width data: *Qp* imaging and inferences on the thermal state of the campi flegrei caldera (southern Italy) *J. Geoph. Res.*
- Del Pezzo, E., De Natale, G., Scarcella, G., Zollo, A., 1987. Qc of three-component seismograms of volcanic micro-earthquakes at Campi Flegrei volcanic area (southern Italy). *Pure and Appl. Geophys.* 123, 685–696.
- De Natale, G., Pingue, F. Ground deformations in collapsed caldera structures. *J. Volc. Geoth. Res.* 57, 19–38.
- De Natale, G., Iannaccone, G., Martini, M., Zollo, A., 1987. Seismic sources and attenuation properties at the Campi Flegrei volcanic area, *Pure Appl. Geophys* 125, 883–917.
- De Natale, G., Pingue, F., Allard, P., Zollo, A., 1991. Geophysical and geochemical modelling of the –1984 unrest phenomena at Campi Flegrei (southern Italy). *J. Volcanol. Geoth. Res.* 48, 199–222.

- De Natale, G., Petrazzuoli, S.M., Pingue, F., 1997. The effect of collapse structures on ground deformation in calderas. *Geoph. Res. Lett.* 24, 1555–1558.
- De Vivo, B., Belkin, H.E., Barbieri, M., Chelini, W., Lattanzi, P., Lima, A., Tolomeo, L., 1989. The Campi Flegrei (Italy) geothermal system: a fluid inclusion study of the Mofete and San Vito fields. *J. Volcanol. Geoth. Res.* 36, 303–326.
- Di Vito, M.A., Isaia, R., Orsi, G., Southon, J., de Vita, S., D'Antonio, M., Pappalardo, L., Piochi, M., 1999. Volcanism and deformation since 12,000 years at the Campi Flegrei caldera (Italy). *J. Volcanol. Geoth. Res.* 91, 221–246.
- Dragoni, M., Magnanensi, C., 1989. Displacement and stress produced by a pressurized, spherical magma chamber, surrounded by a viscoelastic shell. *Phys. Earth Planet. Int.* 56, 316–328.
- Dvorak, J.J., Berrino, G., 1991. Recent ground movement and seismic activity in Campi flegrei, Southern Italy: episodic growth of a resurgent dome. *J. Geophys. Res.* 96, 2309–2323.
- Dvorak, J.J., Gasparini, P., 1991. History of earthquakes and vertical ground movement in Campi Flegrei caldera, Southern Italy: comparison of precursor events to the A.D. eruption of monte Nuovo and of activity since 1968. *J. Volcanol. Geoth. Res.* 48, 77–92.
- Dvorak, J., Mastrolorenzo, G., 1991. History of vertical movement in Pozzuoli Bay, southern Italy: the result of regional extension related to the evolution of the Thyrrenian sea and of local volcanic activity. *GSA special paper.*
- Ferrucci, F., Hirn, A., De Natale, G., Virieux, J., Mirabile, L., 1992. P-SV conversion at shallow boundary beneath Campi Flegrei caldera (Italy): evidence for the magma chamber. *J. Geoph. Res.* 97, 15251–15359.
- Gaeta, F., De Natale, G., Peluso, F., Mastrolorenzo, G., Castagnolo, D., Troise, C., Pingue, F., Mita, G., Rossano, S., 1998. Genesis and evolution of unrest episodes at Campi Flegrei caldera: the role of thermal-fluid-dynamical processes in the geothermal system. *J. Geoph. Res.* 103, 20921–20933.
- Gladwin, M.T., Stacey, F.D., 1974. Anelastic degradation of acoustic pulses in rock. *Phys. Earth Planet. Int.* 8, 332–336.
- Kampfmann, W., Berckemer, H., 1985. High temperature experiments on the elastic and anelastic behaviour of magmatic rocks. *Phys. Earth Planet. Int.* 40, 223–247.
- Liu, H.-P., Warrick, R.E., Westerlund, J.B., Kayen, E., 1994. In situ measurement of seismic shear-wave absorption in the San Francisco Holocene Bay Mud by the pulse-broadening method. *Bull. Seism. Soc. Am* 84, 62–75.
- Mitchell, B.J., 1995. Anelastic structure and evolution of the continental crust and upper mantle from seismic surface wave attenuation. *Rev. Geophys.* 33, 441–462.
- Nelder, J.A., Mead, R., 1965. A simplex method for function minimization. *Computer J.* 7, 308–313.
- Niccolini, A., 1845. *Descrizione della gran terma puteolana volgarmente detta Tempio di Serapide*, Napoli, National Library Collection, 45pp.
- Oliveri del Castillo, A., Quagliariello, M.T., 1969. Sulla genesi del bradisismo flegreo. *Atti assoc.geofis. Ital.*, Napoli. 1–4 October.
- Orsi, G., De Vita, S., di Vito, M., 1996. The restless, resurgent Campi Flegrei nested caldera (Italy): constraints on its evolution and configuration. *J. Volcanol. Geoth. Res.* 74, 179–214.
- Orsi, G., Petrazzuoli, S.M., Wohletz, K., 1999. Mechanical and thermo-fluid behavior during unrest at the Campi Flegrei caldera (Italy). *J. Volcanol. Geoth. Res.* 91, 453–470.
- Press, W.H., Flannery, B.P., Teukolsky, S.A., Vetterling, W.T., 1994. *Numerical Recipes*. Cambridge University Press, New York.
- Romanowicz, B., 1995. A global tomographic model of shear attenuation in the upper mantle. *J. Geoph. Res.* 100, 12,375–12,394.
- Romanowicz, B., Mitchell, B.J., Romanowicz, B., 1998. Attenuation tomography of the Earth's mantle: a review of current status, in *Q of the Earth: global, regional and laboratory Q studies (special issue)*. *Pure Appl. Geoph.* 153, 257–272.
- Sanders, C.O., Nixon, L.D., 1995. S wave attenuation structure in Long Valley caldera, California, from three component S-to-P amplitude ratio data. *J. Geophys. Res.* 100 (12), 12,395–12,404.
- Sanders, C.O., Ponko, S.C., Nixon, L.D., Schwartz, E.A., 1995. Seismological evidence for magmatic and hydrothermal structure in Long Valley caldera from local earthquake attenuation and velocity tomography. *J. Geophys. Res.* 100, 8311–8326.
- Sato, T., Hirasawa, T., 1973. Body wave spectra from propagating shear cracks. *J. Phys. Earth* 21, 415–432.

- Sato, H., Sacks, I.S., 1989. Anelasticity and thermal structure of the oceanic upper mantle: temperature calibration with heat flow data. *J. Geophys. Res.* 94, 5705–5715.
- Troise, C., 1999. Un modello termomeccanico dei Campi Flegrei, PhD Thesis, University of Naples. National Libraries of Rome and Florence, Italy.
- Vasco, D.W., Johnson, L.R., 1998. Whole earth structure estimated from seismic arrival times. *J. Geophys. Res.* 103, 2633–2672.
- Wohletz, K., Civetta, L., Orsi, G., 1999. Thermal evolution of the Phlegraean magmatic system. *J. Volcanol. Geoth. Res.* 91, 381–414.
- Wu, H., Lees, M., 1996. Attenuation structure of Coso geothermal area, California, from wave pulse widths. *Bull. Seism. Soc. Am.* 86, 1574–1590.
- Yokoyama, I., 1971. Pozzuoli event in 1970. *Nature* 229, 532–533.
- Zollo, A., de Lorenzo, S., in. Source parameters and 3-D attenuation structure from the inversion of microearthquake pulse width data: methods and synthetic tests. *J. Geoph. Res.press.*
- Zucca, J.J., Hutchings, L.J., Kasameyer, P.W., 1994. Seismic velocity and attenuation structure of the Geysers Geothermal Field, California. *Geothermics* 23, 111–126.